VOL. 10, NO. 15, AUGUST 2015 ISSN 1819-6608
ARPN Journal of Engineering and Applied Sciences

www.arpnjournals.com

BIOMECHANICAL EFFECTS OF BALLOON KYPHOPLASTY ON TREATED AND ADJACENT NON-TREATED VERTEBRAL BODIES: PRE AND POST OPERATIVE EVALUATION

Muhammad Hazli Mazlan[1], Mitsugu Todo[2], Hiromitsu Takano[3] and Ikuho Yonezawa[3]
[1]Interdisciplinary Graduate School of Engineering Sciences, Kyushu University, Japan
[1]Faculty of Electrical and Electronic Engineering, Universiti Tun Hussein Onn Malaysia, Malaysia
[2]Research Institute for Applied Mechanics, Kyushu University, Japan
[3]Department of Orthopedic Surgery, Juntendo University, Japan
E-Mail: hazli.010@s.kyushu-u.ac.jp

ABSTRACT

Balloon kyphoplasty (BKP) is one of the most reliable minimally invasive surgery (MIS) procedure to treat osteoporotic vertebral compression fractures (VCFs). However, untoward complications of high incidence of adjacent vertebral fractures after BKP and their risk factors are still equivocal. To further investigate the underlying cause of this phenomenon, non-linear finite element analysis (FEA) was fully utilized based on load sharing distribution, strain energy distribution and fracture risks evaluation. For this purpose, an image-based pre and postoperative three-dimensional (3D) finite element models of thoracic and lumbar spinal unit (T11-L3) for an osteoporotic patient were developed. After BKP, the load sharing distribution (between anterior and posterior column), strength and stiffness of the augmented vertebra has significantly improved. However, higher generation of interface stresses and deformation energy were found immediately at the adjacent vertebral bodies, which makes them susceptible to the risks of bone failures. Failure risks evaluation based on the incremented loads of 1kN to 10kN (50% risk of spinal injury) have shown very encouraging results. Apparently, the postoperative deformation onset loading (5kN) was fallen within the acceptable range that was higher than the standard normal daily living activities (1kN). It is believed that, the optimization of the material properties used in BKP procedure with the depth understanding on the historical and natural evolution of the osteoporosis could achieve optimal clinical outcomes in the future.

Keywords: balloon kyphoplasty, vertebral compression fractures, finite element analysis.

INTRODUCTION

Vertebral compression fractures (VCFs) has become a global issue in relation to the improved healthcare and lifestyle. The underlying cause of this disease might be due to trauma, disease of the spine and the most common cause is osteoporosis. The clinical significance of osteoporotic lies in its high vulnerability and susceptibility to bone fractures (Homingga *et al.*, 2004), and the most prevalent fracture site is the spine (Melton and Chrischillies, 1992). It is characterized by the low bone mass and micro-architectural deterioration of the bone tissues (Peck *et al.*, 1993). It has been reported that two-thirds of VCFs was detected asymptomatically (Cooper, O'Neill and Silman, 1993) and if left untreated VCFs would increase the chance of subsequent fractures by 500% leading to a dramatic health deterioration and perhaps increase the risk of mortality (Mathis *et al.*, 2001). In Japan, there are more than 10 million osteoporosis patients (Tawara *et al.*, 2006). It is believed that this number will significantly increase in relation to Japan's life expectancy continues to rise.

Minimal invasive surgery (MIS) procedure of balloon kyphoplasty (BKP) is of the most reliable treatment to treat VCFs disease. BKP requires the injection of bone cement into the vertebrae in order to stabilize fractured vertebrae, restore the height of the compressed vertebral body, relieve pain, reduce the incidence of cement leakage into spinal canal, correct kyphosis deformities, and achieve a fully spinal functional outcomes (Zhang *et al.*, 2010). Apparently, the selection of the bone cement as a filling material play the utmost role in determining the effectiveness of the treatment (He *et al.*, 2015). Basically, the bone cement must have the considerable mechanical strength and toughness, they must be radiopaque under fluoroscopy, and they should have an adequate viscosity and be injectable for facilitating BKP procedure (He *et al.*, 2015), (Zhang *et al.*, 2010), (Lavelle and Cheney, 2006). Many reports have shown clinical improvements for patient treated with BKP (Luo, Adams and Dolan, 2010). However, recurrent vertebral compression fractures, particularly at the adjacent levels has been raising consternation about its further complications.

The objectives of this study were to quantitatively analyze the load transfer mechanisms of pre and postoperative models of patient with VCFs treated with BKP procedures. It was also to investigate to what extent would BKP procedures increase the strength and stiffness of the treated vertebra and concurrently induce the occurrence of VCFs at the adjacent non-treated vertebrae level.

MATERIALS AND METHODS

FE modeling

Three-dimensional FE models of pre and

postoperative vertebrae column (T12-L3) of an osteoporotic patient (Figure-1) were constructed in MECHANICAL FINDER™ software (Research Center of Computational Mechanics Co. Ltd. Japan). Written informed consent, permission and cooperation of 74-year-old Japanese female osteoporotic patient was obtained. To create the FE models, CT scan images of the osteoporotic subjects (Department of Orthopedic Surgery, Juntendo University, Japan) were taken pre and postoperatively and transferred to FE software. From the obtained CT scan images, the FE models were then constructed based on the extracted bone edges of the region of interests (ROI) around the outer region of the cortical bone to obtain the anatomical structure of the spinal bone. The same process was also repeated in order to obtain the physical structure of the augmented bone cement in the postoperative model. The FE models were then modelled with 1mm linear tetrahedral and triangular elements. The tetrahedral element was used to represent the bone cement and the inner portion of the cortical and cancellous bone. The triangular element with the thickness of 0.4mm was used to represent the outer cortex.

To reflect the heterogeneity of the FE models, the mechanical properties for each element were calculated from the Hounsfield Unit (HU) values. Young's modulus of each element were obtained using the relationship as reported by Keyak *et al.* (1998). Poisson's ratio was set to a constant value of 0.4 (Keyak *et al.*, 1998), (Reilly and Burstein, 1975), (Van Burskik and Ashman, 1981). Facet joint cartilages and intervertebral discs were created based on the approximation and visualization of their actual structure and position that were verified by orthopaedic surgeons. Poisson's ratio for the intervertebral discs and the facet joint cartilages were set at 0.45 and 0.2, correspondingly. Meanwhile, the young's modulus were set at 8.4MPa and 11MPa, respectively (Table-1). The material properties of the bone cement are listed in Table-2.

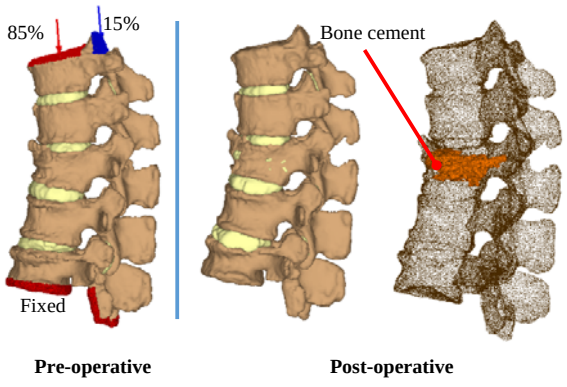

Figure-1. Pre and postoperative models. The same loads and boundary conditions were applied to the both model.

Table-1. Facet joint cartilages and intervertebral disc material properties.

Material	Young's Modulus (MPa)	Poisson's Ratio
Intervertebral Disc	8.4	0.45
Facet Joint	11	0.2

Table-2. Bone cement material properties (Kurtz, Villarragaa and Zhao, 2005(a)), (Kurtz, Villarragaa and Zhao, 2005(b)).

Material properties	Bone cement
Poisson's ratio	3.7
Young's modulus	3700MPa
Critical strength	31MPa
Yield strength	111MPa

Analysis

The FE models were loaded with compressive loading of 1kN (Tawara *et al.*, 2006), (Mazlan et al, 2014). The load was then incrementally increased up to 10kN in order to evaluate the failure risks in the vertebrae. The 10kN compressive/impact loading was used to simulate the worst loading condition, the force at which there is 50% risk of injury (Meyerhoff *et al.*, 2008). The loadings were applied to the superior surface of T11, while the inferior surface of L3 was fixed in all directions (Figure 1). The loads were modeled according to the three-column load distribution (85% of the load was applied to the vertebral body, 15% to the neural arch) (Zhang *et al.*, 2010).

The biomechanical effects of the pre and postoperative models were thoroughly analyzed and investigated based on the non-linear finite element analysis. The analysis was focused on the load sharing distribution at the anterior and posterior column of the vertebrae, and the interface stresses at the intervertebral disc-endplate and facet joint cartilage junction. In addition, the strain energy distribution (SED) variations were also investigated. The SED was obtained from the principle stress and stress invariant (Chiang and Wang, 2006). It was reported that the load transmission mechanism of the SED can be used as a failure criterion of an element.

The fracture risks evaluation of the vertebrae were analyzed based on the Newton-Raphson method (Bessho *et al.*, 2007), (Tawara *et al.*, 2014). The analysis were translated into a graphical representation of failure and yielding element distributions. The criteria of the failure elements were divided into compressive and tensile directions. The initiation of the failure in a tensile direction was initiated when the maximum principle stress is higher than the ultimate tensile stress. The ultimate tensile stress was set as 80% of the compressive yield stress. As for the compressive direction, the failure criteria was divided into two stages according to Drucker-Prager yield criterion. The first stage known as a yielded state and it occurs when the Drucker-Prager equivalent stress

exceeds the compressive yield stress. The second stage or the state of the initiation of failure commences when the minimum principle strain of an element is less than -10000 microstrains in a yielded state.

RESULTS AND DISCUSSIONS

Drucker-Prager stress distribution for the pre and postoperative models under the application of 1kN compressive loading are shown in Figure-2. In general, the Drucker-Prager stress of the postoperative model was distributed more evenly than the preoperative model. This condition was closely related to the failure of the intervertebral disc to distribute the compressive stress evenly on the adjacent vertebral bodies preoperatively. By implementing the BKP procedure, the disc pressure could be restored back to normal and the stress could be distributed more evenly on the adjacent vertebral bodies. Obviously, for the treated L1 vertebra, the highest stress concentration could be found at the interface between the bone cement and the cancellous bone junction. This condition might be related to the stiffness mismatch between the bone cement and the cancellous bone, which might cause bone resorption in the long run (Mazlan *et al.*, 2014). This condition could be reduced by enhancing the bone cement material properties to the value that is close to the cancellous bone material properties with improved mechanical strength and stiffness.

Figure-3 shows the stress distribution between the anterior (vertebral body) and posterior column (neural arch) of the vertebrae. Obviously, BKP has significantly reduced the stress concentration gap between the two segments especially at the L1 vertebra. The neural arch load bearing for the postoperative model at the L1 and L2 experienced lower stress concentration than the pre-operative model. The most affected region was at the pedicle region of the L1 vertebra as depicted in Figure-2. However, the risk of the bone failure was still exist at the T12 vertebra based on the high stress concentration gap difference postoperatively. This is based on the fact that, the high stress concentration gap between the neural arch and vertebral body might cause the area with lower stress concentration would be stress shielded, reducing the bone density and finally increased the risk of bone failures (Luo, Adams and Dolan, 2010). It has to be borne in mind that, it is also not good to have a high stress concentration on the anterior column of the vertebra, since the anterior column is more susceptible to damage due to its low bone mineral density especially in elderly spine (Lavelle and Cheney, 2006).

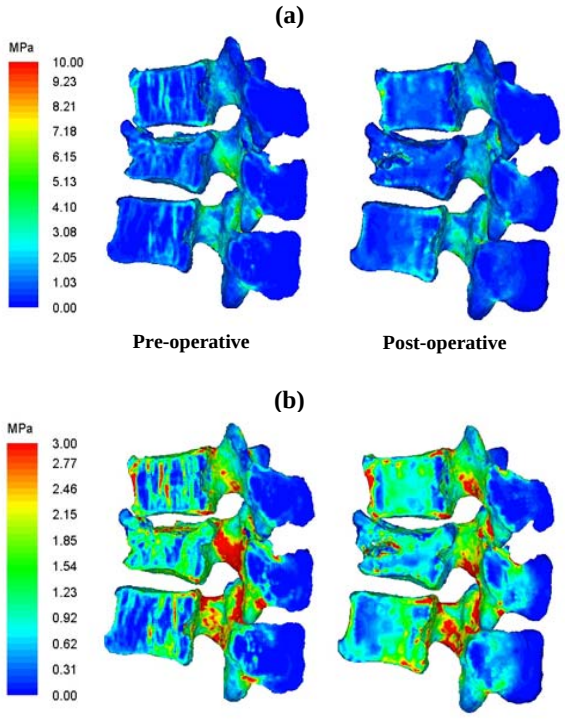

Figure-2. Drucker-Prager stress distribution mapped at (a) ordinary and (b) down-sized scale.

Table-3 and Table-4 show the distribution of the Maximal Drucker-Prager stress at disc-endplates and facet joints junctions, respectively. Obviously, after BKP surgery, the maximum L1 superior and inferior endplates Drucker-Prager stresses increased by 27.27% and 96.5%, respectively. However, at the adjacent non-treated vertebrae two contradictory results were observed. The maximum T12 inferior endplate Drucker-Prager stress decreased by 16.46%, while the maximum L2 superior endplate increased by 48.98%. The reduction of the maximal Drucker-Prager stress at the T12 endplate was compensated with the increased of the stress at the T12 inferior articular facet, while the increment of the maximal Drucker-Prager stress at the L2 superior endplate was compensated with the decrease of the stress at the L2 superior articular facet. Obviously, after BKP the interface stresses (inferior and superior endplates) at the treated vertebra has increased significantly and therefore the adjacent non-treated vertebrae has to absorb the higher load impacts produced at this region. This showed that the bone cement has increased the total strength and stiffness level of the treated vertebra and thus increasing the stress on the endplates immediately above and below the treated vertebral body, leading to increase pressure on the adjacent discs, and eventually producing higher stress on the endplate of the adjacent vertebrae (Zhang *et al.*, 2010), (Luo, Adams and Dolan, 2010).

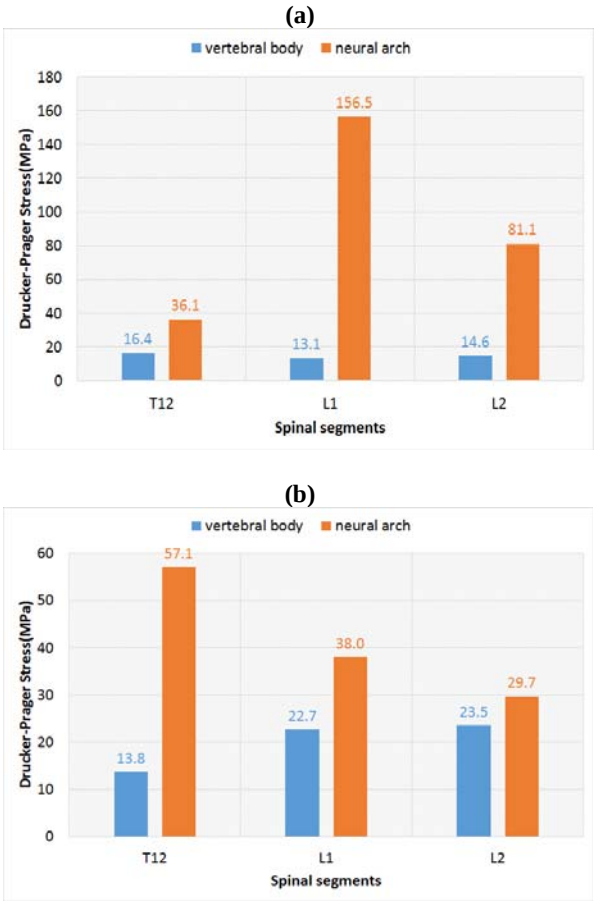

Figure-3. Graph of Maximal Drucker-Prager stress distribution at the anterior and posterior column for the (a) pre and (b) postoperative models.

Table-3. Maximal Drucker-Prager interface stress at disc-endplates junction.

	Pre-operative	Post-operative	Percentage difference
T12 inferior endplate	12.9	10.8	-16.5%
L1 superior endplate	13.1	16.7	27.3%
L1 inferior endplate	8.5	16.7	96.5%
L2 superior endplate	13.5	20.1	49.0%

Table-4. Maximal Drucker-Prager interface stress at the facet joint cartilages junction.

	Pre-operative	Post-operative	Percentage difference
T12 inferior articular facet	16.5	150.7	811.3%
L1 superior articular facet	19.2	76.2	296.9%
L1 inferior articular facet	314.3	45.4	-85.6%
L2 superior articular facet	54.5	43.6	-20.0%

SED variations as shown in Figure-4 and Figure-5 is one of a reliable method to interpret the load transfer mechanism and the risk of bone fractures in vertebrae. For the both cases (pre and postoperative models) the adjacent non-fractured and non-treated vertebrae experienced higher SED than the fractured and treated vertebra. Since the input energy of the motion segment was remained the same, therefore the adjacent non-treated and non-fractured vertebrae have to absorb the extra energy and hence increases the risk of vertebral bone failures. For the postoperative model, the strain energy density at the L1 has been significantly reduced and the risk of fracture at this area was assumed reduced. By virtue of the potential energy stored in a volume, the SED is reflecting the amount of work that has to be done to produce the elastic deformation (Chiang and Wang, 2006). Therefore, this mechanism could be used as a tool to predict which area of the vertebral bodies that are susceptible to vertebral failures based on this energy type failure criterion (Li, 2001). In addition, the results showed that the adjacent non-treated vertebrae were weaker and less stiff than those treated with BKP. This mechanism may explain the clinical observation of the adjacent vertebral failure after BKP.

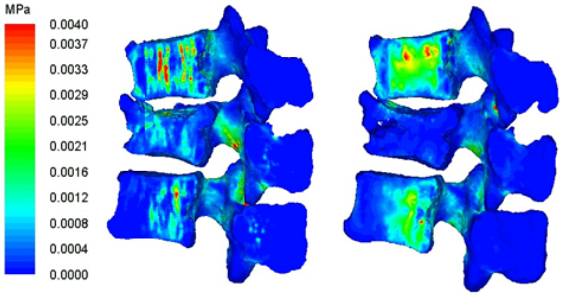

Figure-4. Strain energy density distribution.

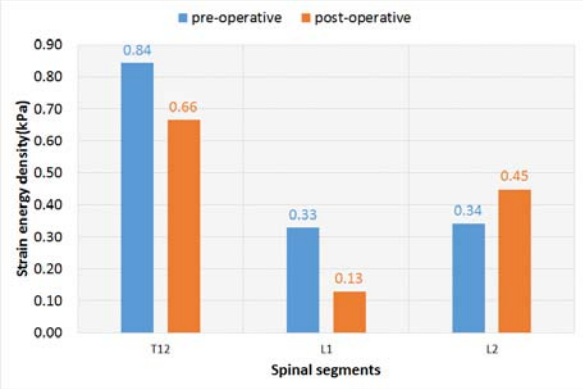

Figure-5. Graph of strain energy density distribution at the anterior and posterior column.

To further enhance the investigation on the phenomenon of the adjacent non-treated vertebral fractures, bone fracture analysis based on the Newton-Raphson method was applied. The distribution of the failure and yielding shell elements in tensile and compressive directions under the incremented compressive loading of 1kN to 10kN are given in Figure-6. Apparently, the initiation of element failure was started to show its significant impact when the load was increased from 7kN to 10kN. The amount of failure and yielding shell elements at the adjacent non-treated vertebrae T12 and L2 were comparably higher for the postoperative than the preoperative model. However, at the treated vertebra L1 the number of the yielding and failure elements has decreased postoperatively as described in Figure-6(b). These phenomena were believed to have a strong relationship with the improved mechanical properties of the treated vertebra. As a result, the fractures were initiated at the adjacent vertebral bodies. This situation could be translated into a graphical representation as depicted in Figure-7. The fracture of the vertebrae were defined as occurring when at least one shell element failed. Therefore, it was comprehensively understood that these results will be highly reflected its clinical outcomes in a real situation (Bessho *et al.* 2007).

(a)

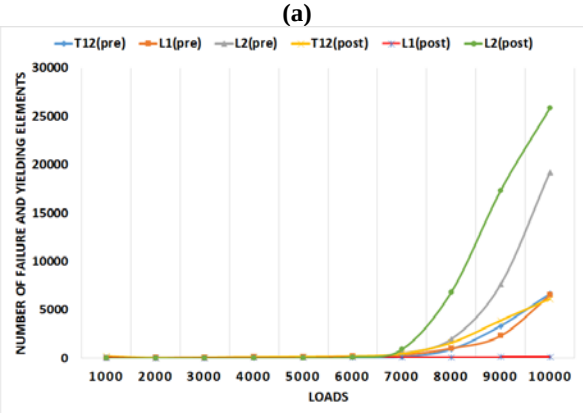

(b)

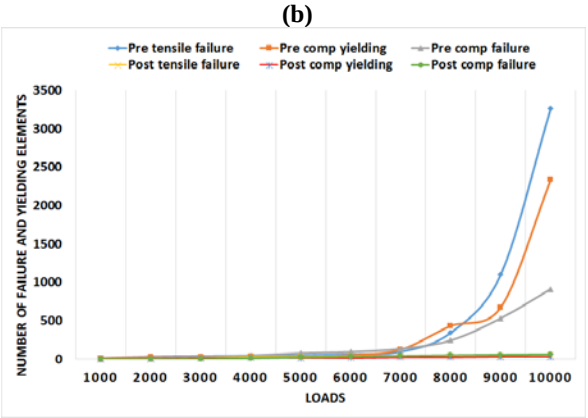

Figure-6. Historical changes in the number of shell elements having undergone tensile failure, compressive yielding and compressive failure under the application of incremented loading of 1kN to 10kN.

(a)

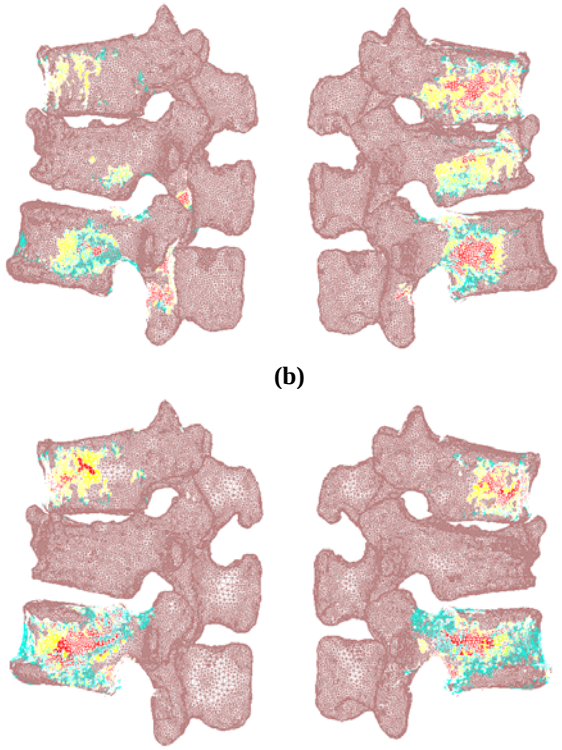

(b)

Figure-7. Distribution of failure and yielding shell elements under the application of 10kN (a) pre and (b) postoperative models.

The Finite element analysis have shown a very significant impact on the evaluation of BKP procedures. The adverse effect of the VCFs in osteoporotic and elderly people is well understood (Uppin *et al.* 2003). Spinal deformity biomechanically produced uneven high stress and strain distributions leading to the initiation of subsequent fractures even with a normal daily living

activities (Mazlan *et al.* 2014). Postoperative results has shown that BKP has significantly improved the load sharing distributions between the anterior and the posterior vertebral coulmn and tremendously increased the stiffness and strength of the fractured vertebral body towards prefracture levels. Moreover, the onset load for the initation of the failure and yielding elements at the treated vertebral level of L1 was significantly improved in comparison to the preoperative model. As for the fractured vertebra, the onset load could be detected as early as 5kN, whereas for the treated vertebra only microdamages were detected at the maximum load of 10kN. Generally, after BKP surgery, bone damage formation was started to occur under the impact loading of 7kN. This condition is mechanically acceptable since the onset load was much more higher than the normal daily living activities as reported by Han *et al.*2013. However, the bone failure risks was still exist at higher load and therefore high risks activity must be completely avoided. Inevitable events such as falling or accidents might still have imposed high susceptibility of bone failure either on the treated or non-treated vertebrae.

Despite its superior characteristic in improving the mechanical properties of the fratured vertebra, the result has suggested that BKP could increase the stress on the endpates immediately above and below it, and hence producing higher stress on the adjacent vertebral endplates, which then putting them in a state of bone failures. It has also shown that the results of the SED load transfer mechanisms (Chiang and Wang, 2006) was correlated well with the results of the failure analysis utilizing by Newton-Raphson method (Bessho *et al.* 2007), (Tawara *et al.* 2014). Eventhough the main contributing factors of this phenomenon is still equivocal, we are strongly believed that a few factors like the type and amount of the injected bone cement, bone loss and natural evolution of osteoporosis on the spine were underlying the cause of this problem (Uppin *et al.* 2003) (Luo, Adams and Dolan, 2010), (Zhang *et al.* 2010), (He *et al.* 2011) (He *et al.* 2015). In a related study, bone cement leakage into veretebral disc was detected as one of the confounding factors that increases the risk of a new fracture at the adjacent vertebral bodies (Lin *et al.* 2004). In addition, rapid clinical improvement postoperatively might cause the patient to be able to get involve in more active activities that they were unable to do it previously. Eventhough they may resume fully recovery, the new axial load on the veretbra may be stressful and leading to a new compression fractures on the adjacent vertebrae (Uppin *et al.* 2003).

Improving mechanical properties of the bone cement has been one of the main focus in optimizing the usage of the materials in BKP development. Biomechanically, the bone cement must be have an adequate stiffness, compressive, shear and tensile strength in order to avoid massive biomechanical alteration of the spine (Zhang *et al.* 2010), (He *et al.* 2015). Besides, the bone cement choices must be based on comprehensive mechanical consideration to be able to be well adapted to the natural environment of the spinal bone (Verlan, Oner and Dhert, 2006). Moreover, being able to simultaneuosly promote bone formation yet suppress bone resorption is an added advantage for a promising type of bone cement utilizes in BKP procedure (He *et al.* 2015). Thus, the recurrent VCFs at the adjacent non-treated vertebrae could be highly avoided in the future.

CONCLUSIONS

FEA studies have shown that BKP procedure on the osteoporotic patient has significantly improved the biomechanical outcomes of the treated and non-treated vertebral bodies. Moreover, the postoperative deformation onset loading was fallen within the acceptable range that was higher than the normal daily living activities. The phenomenon of high incidence of adjacent vertebral bone failures could be well understood and showed very encouraging results. Therefore, the complimentary mechanisms of the stress distribution, SED distribution and non-linear fracture analysis could be used as reliable tools to predict and investigate the effectiveness of the given surgical procedure.

ACKNOWLEDGEMENT

This research was partially supported by The Ministry of Education Malaysia.

REFERENCES

[1] Bessho M., Ohnishi I., Matsuyama J., Matsumoto T., Imai K. and Nakamura K. 2007. Prediction of strength and strain of the proximal femur by a CT-based finite element method. Journal of Biomechanics, 40, pp. 1745-1753.

[2] Chiang C.-K. and Wang J.-L. 2006. Strain energy density variations of osteoporotic spine column after bone cement augmentation – an invitro porcine biomechanical model. Journal of Biomechanics, 39(sppl 1), S150.

[3] Cooper C., O'Neill T. and Silman A. 1993. The epidemiology of vertebral fractures. European vertebral osteoporosis study group, Bone, Vol. 14, No. 1, pp. 89-97.

[4] Keyak J.H., Rossi S.A., Jones K.A. and Skinner H.B. 1998. Prediction of femoral fracture load using automated finite element modeling. Journal of Biomechanics, Vol. 31, No. 2, pp. 125-133.

[5] Han K.S., Rohlmann A., Zander T. and Taylor W.R. 2013. Lumbar spinal loads vary with body height and weight. Medical Engineering and Physics, Vol. 35, No. 7, pp. 969-977.

[6] He Z., Zhai Q., Hu M., Cao C., Wang J., Yang H. and Li B. 2015. Bone cements for percutaneous vertebroplasty and balloon kyphoplasty: Current

status and future developments. Journal of Orthopaedic Translation, Vol. 3, No. 1, pp. 1-11.

[7] Homminga J., Van-Rietbergen B., Lochmuller E.M., Weinans H., Eckstein F. and Huiskes R. 2004. The osteoporotic vertebral structure is well adapted to the loads of daily life, but not too infrequent ''error'' loads", Journal of Bone, Vol. 34, No. 3, pp. 510-516.

[8] Kurtz S.M., Villarragaa M.L., Zhao K. and Edidin A.A. 2005(a). Static and fatigue mechanical behavior of bone cement with elevated barium sulfate content for treatment of vertebral compression fractures, Journal of Biomaterials, 26, pp. 5926.

[9] Kurtz S.M., Villarragaa M.L., Zhao K. and Edidin A.A. Erratum to Static and fatigue mechanical behavior of bone cement with elevated barium sulfate content for treatment of vertebral compression fractures, Journal of Biomaterials, Vol. 26, pp. 5926, 2005.

[10] Lavelle W.F. and Cheney R. 2006. Recurrent fracture after vertebral kyphoplasty. The Spine Journal, Vol. 6, No. 5, pp. 488-493.

[11] Li Q.M. 2001. Strain energy density failure criteria. International Journal of Solids and Structures, 38, pp. 6997-7013.

[12] Lin E.P., Ekhlom S., Hiwatashi A. and Westesson P.L. 2004. Vertebroplasty: Cement leakage into the disc increases the risk of new fracture of adjacent vertebral body. American Journal of Neuroradiology, Vol. 25, No. 2, pp.175-180.

[13] Luo J., Adams M.A. and Dolan P. 2010. Vertebroplasty and Kyphoplasty can restore normal spine mechanics following osteoporotic vertebral fracture. Journal of Osteoporosis [Online]. Id 729257.

[14] Mathis J.M., Barr J.D., Belkoff S.M., Barr M.S., Jensen M.E. and Deramond H. 2001. Per-cutaneous vertebroplasty: a developing standard of care for vertebral compression fractures. , American Journal of neuroradiology, Vol. 22, pp. 373-381.

[15] Mazlan M.H., Todo M., Takano H. and Yonezawa I. 2014. Finite element analysis of osteoporotic vertebrae with first lumbar (L1) vertebral compression fracture. International Journal of Applied Physics and Mathematics, Vol. 4, No. 4, pp. 267-274.

[16] Melton L.J., Chrischilles E.A., Cooper C., Lane A.W. and Riggs B.L. 1992. Perspective. How many women has osteoporosis? Journal of Bone and Mineral Research, Vol. 7, No. 9, pp. 1005-1010.

[17] Meyerhoff K., Planchak C., Damon A. and Bass G.T. 2008. Thoracic and lumbar spinal impact tolerance. Accident Analysis and Prevention, Vol. 40, No. 2, pp. 487-495.

[18] Peck W.A., Burckhardt P., Christiansen C. *et al*. 1993. Consensus development conference: diagnosis, prophylaxis, and treatment of osteoporosis. American Journal of Medicine, Vol. 94, No. 6, pp. 646–650.

[19] Reilly D. T. and Burstein A.H. 1975. The elastic and ultimate properties of compact bone tissue. Journal of Biomechanics, Vol. 8, No. 6, pp. 393-405.

[20] Tawara D., Noro K., Tsujikami T., Okamoto Y. and Murakami H. 2014. Nonlinear mechanical analysis of posterior spinal instrumentation for osteoporotic vertebra: effects of mechanical properties of the rod on the failure risks around the screw. Journal of Biomechanical Science and Engineering (advanced publication 2014).

[21] Tawara D., Sakamoto J., Kanazawa H., Sekimoto A., Awamori S., Murakami H., Kawahara N., Oda J. and Tomita K. 2006. Investigation of vertebral fracture risks in osteoporosis by patient-specific finite element analysis. Transactions of the Japan Society of Mechanical Engineers Series A, 72, pp. 255-262.

[22] Uppin A.A., Hirsch J.A., Centenera L.V., Pfiefer B.A., Pazianos A.G. and Choi I.S. 2003. Radiology, Vol. 226, No. 1, pp. 119-124.

[23] Van Buskirk W.C. and Ashman R.B. 1981. The elastic moduli of bone. Trans. American Society of Mechanical Engineers (Applied Mechanics Division), 45, pp. 131-143.

[24] Verlan J.J., Oner F.C. and Dhert W.J. 2006. Anterior spinal column augmentation with injectable bone cements. Biomaterials for Spinal Applications, Vol. 27, No. 3, pp. 290-301.

[25] Zhang L., Yang G., Wu L. and Yu B. 2010. The biomechanical effects of osteoporosis vertebral augmentation with cancellous bone granules or bone cement on treated and non-treated vertebral bodies: A finite element evaluation, Clinical Biomechanics, Vol. 25, No. 2, pp. 166-172.